First Measurements of Form Factors of Pion, Kaon, Proton, and Hyperons for the Highest Timelike Momentum Transfers

Kamal K. Seth

Northwestern University, Evanston, IL, 60208, USA

E-mail: kseth@northwestern.edu

Abstract. Results of recent precision measurements of the electromagnetic form factors of the pion, kaon, proton, and the hyperons, Λ^0, Σ^0, Σ^+, Ξ^-, Ξ^0, Ω^-, at large timelike momentum transfers are presented. Evidence is found for diquark correlations in Λ^0, Σ^0 hyperons.

With the discovery of quarks hadrons were recognized as composite. It is generally agreed that electromagnetic form factors at large momentum transfer provide some of the best insight into the structure of the composite hadron. Four-momentum transfers defined as

$$Q^2(4\text{ mom}) = q^2(3\text{ mom})_{\text{space}} - (\text{energy})_{\text{time}}$$

can be *positive and spacelike*, or *negative and timelike*. I am going to talk about form factors for timelike momentum transfers as measured via the reactions $e^+e^- \to \text{hadron} - \text{antihadron}$.

In 1960, in anticipation of electron-positron colliders, Cabibbo and Gatto wrote two classic papers [1] pointing out that these colliders would provide the unique opportunity to measure timelike form factors of any hadrons, mesons and baryons. Only 50 years later, we are now realizing the full promise of the vision of Cabibbo and Gatto in the measurements I am reporting here.

Before 2000 almost no experimental data with any precision existed for any hadron for timelike form factors for $|Q^2| > 5$ GeV^2. Recently, we made the first measurements of the form factors of pions, kaons, and protons with high precision for the large momentum transfers of $|Q^2| = 14.2$ and 17.4 GeV^2 [2].

The important results of these measurements are presented in Table 1 and Fig. 1 are:

(i) There is a remarkable agreement of the form factors with the dimensional counting rule prediction of QCD, that $|Q^2|F_{\pi,K}$ and $|Q^4|F_p$ are nearly constant, varying with $|Q^2|$ only weakly as $\alpha_S(|Q^2|)$ and $\alpha_S^2(|Q^2|)$. There is, however, an unexpected departure for protons at $|Q^2| = 14.2$ GeV^2.

(ii) The theoretical predictions for the magnitudes of $F_\pi(|Q^2|)$ and $F_p(|Q^2|)$ fail by factors, ≥ 2.

(iii) While pQCD predicts that $F_\pi/F_K = (f_\pi/f_K)2 = 0.67 \pm 0.01$, we find:

$$F_\pi/F_K = 1.21 \pm 0.03, \text{ at } |Q^2| = 14.2\text{GeV}^2, \quad F_\pi/F_K = 1.09 \pm 0.04, \text{ at } |Q^2| = 17.4\text{GeV}^2.$$

It has been suggested that this dramatic disagreement may be due to the kaon wave function being different from that of the pion due to $SU(3)$ breaking, the strange quark in the kaon

having a 27 times larger mass than the up/down quarks in the pion. However, recent lattice calculations do not support this conjecture.

Table 1. Results for pion, kaon and proton timelike form factors.

Q^2 (GeV^2)	$Q^2 F_\pi(\lvert Q^2\rvert)$ (GeV^2)	$Q^2 F_K(\lvert Q^2\rvert)$ (GeV^2)	$Q^4 F_p(\lvert Q^2\rvert)/\mu_p$ (GeV^4)
14.2	0.92 ± 0.04	0.76 ± 0.02	0.64(3)
17.4	0.84 ± 0.03	0.77 ± 0.03	0.82(5)

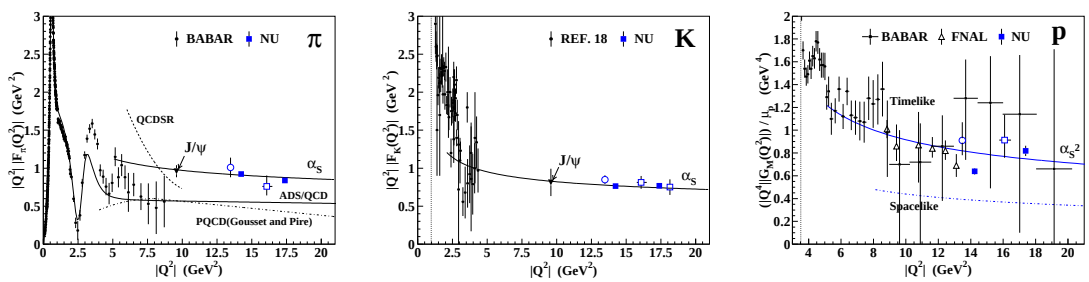

Figure 1. Results for pion, kaon and proton timelike form factors.

In the context of the quark-gluon structure of hadrons, it is particularly interesting to measure form factors of hyperons which may be expected to reveal the effects of $SU(3)$ breaking as successively one, two, and three of the up/down quarks in the nucleon are replaced by strange quarks in (Λ, Σ), Ξ, and Ω, respectively. The interest is further enhanced at large momentum transfers at which deeper insight is obtained into possible short-range correlations between the quarks. As Wilczek [4] has pointed out, "several of the most profound aspects of low-energy QCD dynamics are connected to diquark correlations," and the differences in quark-quark configurations between different hyperons make them an ideal laboratory to study diquark correlations.

The $e^+e^- \to$ hyperon $-$ antihyperon cross sections were expected to be very small, and no experimental measurements were reported for 47 years after Cabibbo and Gatto's papers. In 2007, BaBar reported [3] form factor measurements for Λ and Σ^0 using the ISR method, but with statistically significant results were limited to $|Q^2| \lesssim 6$ GeV^2. Now we have measured form factors of all hyperons, Λ^0, Σ^0, Σ^+, Ξ^-, Ξ^0, Ω^- for the first time with good precision at the large momentum transfer of $|Q^2| = 14.2$ GeV^2.

The only existing theoretical study of hyperon form factors at large timelike momentum transfers is due to Körner and Kuroda [5]. These predictions were not constrained by any experimental measurements, and they turn out to be factors 10 to 80 larger than what we measure.

We use data taken with the CLEO-c detector at $\psi(3770)$, $\sqrt{s} = 3.77$ GeV, with the integrated luminosity $\mathcal{L} = 805$ pb^{-1}. Data taken at $\psi(3770)$ can only be used to determine hyperon form factors if it can be shown that the strong interaction yield of the hyperons at the $\psi(3770)$ resonance is negligible. We estimate it by using the pQCD prediction that the ratios of the branching fractions for the decay of any two vector resonances of charmonium to leptons (via virtual photons) and hadrons (via gluons) are identical. This relation leads to the estimates that the expected number of events for resonance decays of $\psi(3770)$ in our measurements are 1.3 p, 0.9 Λ^0, 0.2 Σ^+, Σ^0, Ξ^-, 0.05 Ξ^0, and 0.03 Ω^-. In other words, the contributions of strong decays are negligibly small in all decays, and the observed events arise from form factor decays.

We also use CLEO-c data taken at $\psi(2S)$, $\sqrt{s} = 3.686$ GeV, with luminosity $\mathcal{L} = 48$ pb^{-1}, which corresponds to $N(\psi(2S)) = 24.5 \times 10^6$, to measure the branching fractions for the decays $\psi(2S) \to B\overline{B}$. The large yield from resonance production of $B\overline{B}$ pairs from $\psi(2S)$ enables us to test the quality of our event selection criteria, and to determine contributions to systematic uncertainties.

We reconstruct the hyperons in their following major decay modes (with branching fractions [7] listed in parentheses): $\Lambda^0 \to p\pi^-$ (63.9%), $\Sigma^+ \to p\pi^0$ (51.6%), $\Sigma^0 \to \Lambda^0\gamma$ (100%), $\Xi^- \to \Lambda^0\pi^-$ (99.9%), $\Xi^0 \to \Lambda^0\pi^0$ (99.5%), $\Omega^- \to \Lambda^0 K^-$ (67.8%). We find that reconstructing back-to-back hyperons and anti-hyperons whose decay vertices are separated from the interaction point results in essentially background free spectra. We first identify single hyperons, and then construct hyperon-antihyperon pairs.

To determine the reconstruction efficiency of the above event selections, we generate Monte Carlo events using a GEANT-based detector simulation and the expected angular distribution.

The single hyperon mass spectra for $\psi(2S)$ decays are shown in Fig. 2 (left), for hyperons with $E(B)/E_{\rm beam} > 0.95$. Clear peaks are seen for the reconstructed hyperons.

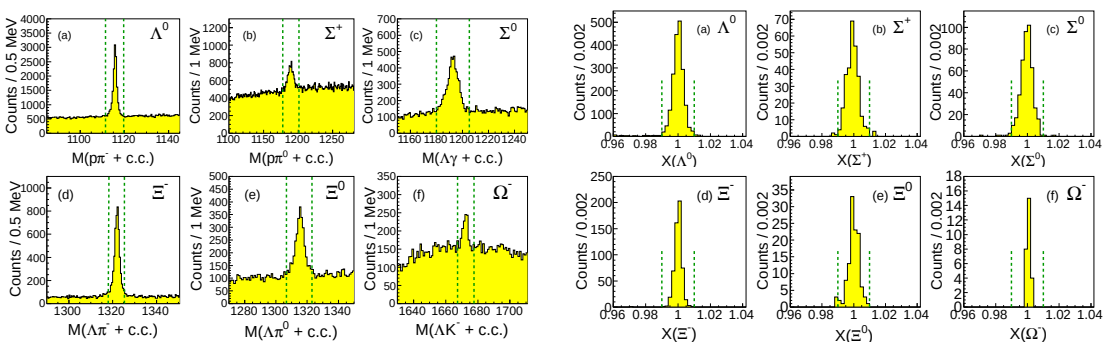

Figure 2. (left) Invariant masses of reconstructed final states in $\psi(2S)$ data. Single hyperons are accepted in the regions defined by vertical dashed lines. (right) Distributions of baryon–antibaryon events as function of, $X(B) \equiv (E(B) + E(\overline{B}))/\sqrt{s}$, in $\psi(2S)$ data. The vertical lines indicate the signal region $X = 0.99 - 1.01$.

The second step of analysis consists of constructing baryon–antibaryon pairs. The distributions of these $B\overline{B}$ pairs is shown in Fig. 2 (right) for $\psi(2S)$ decays as a function of $X(B) \equiv [E(B) + E(\overline{B})]/\sqrt{s}$, which should peak at $X(B) = 1$. Clear peaks are seen for all decays with essentially no background. We define the signal region as $X(B) = 0.99 - 1.01$, with numbers of events in it as $N_{\rm data}$. We calculate the radiative correction, $(1+\delta)$, using the method of Bonneau and Martin [8]. We obtain $(1+\delta) = 0.77$ within 1% for all baryons for both $\psi(2S)$ and $\psi(3770)$. The Born cross sections are calculated as $\sigma_B = N_{\rm data}/\epsilon_B\,\mathcal{L}(\psi(2S))\,(1+\delta)$, and the branching fractions as $\mathcal{B}(\psi(2S) \to B\overline{B}) = N_{\rm data}/\epsilon_B N(\psi(2S))$. The results are summarized in Table 2, including those for $\psi(2S) \to p\bar{p}$. The first uncertainties in σ_B and $\mathcal{B}$ are statistical, and the second uncertainties are estimates of systematic uncertainties. Our results for $\psi(2S)$ branching fractions are in agreement with the PDG averages [7] and previous small luminosity CLEO results [9], and have generally smaller errors.

We apply the same event selections to the $\psi(3770)$ decays as we do for $\psi(2S)$ decays. The $X(B)$ distributions for $\psi(3770)$ form factors decays are shown in Fig. 3 (left). Clear peaks are seen for each decay mode. The number of events, $N_{\rm ff}$, in the region $X(B) = 0.99 - 1.01$, are used to calculate the cross sections as, $\sigma_0(e^+e^- \to B\overline{B}) = N_{\rm ff}/(1+\delta)\epsilon_B\,\mathcal{L}(3770)$, where ϵ_B are the MC-determined efficiencies, and $\mathcal{L}(3770) = 805$ pb^{-1} is the luminosity.

Table 2. Cross section and branching fraction results for $\psi(2S) \to B\overline{B}$.

$\mathcal{B}$	$N_{\rm data}$	ϵ_B (%)	σ_B (pb)	$\mathcal{B} \times 10^4$
p	4475(78)	63.1	196(3)(12)	3.08(5)(18)
Λ^0	1901(44)	20.7	247(6)(15)	3.75(9)(23)
Σ^0	439(21)	7.96	148(7)(11)	2.25(11)(16)
Σ^+	281(17)	4.54	165(10)(11)	2.51(15)(16)
Ξ^-	548(23)	8.37	176(8)(13)	2.66(12)(20)
Ξ^0	112(11)	2.26	135(13)(10)	2.02(19)(15)
Ω^-	27(5)	2.32	31(6)(3)	0.47(9)(5)

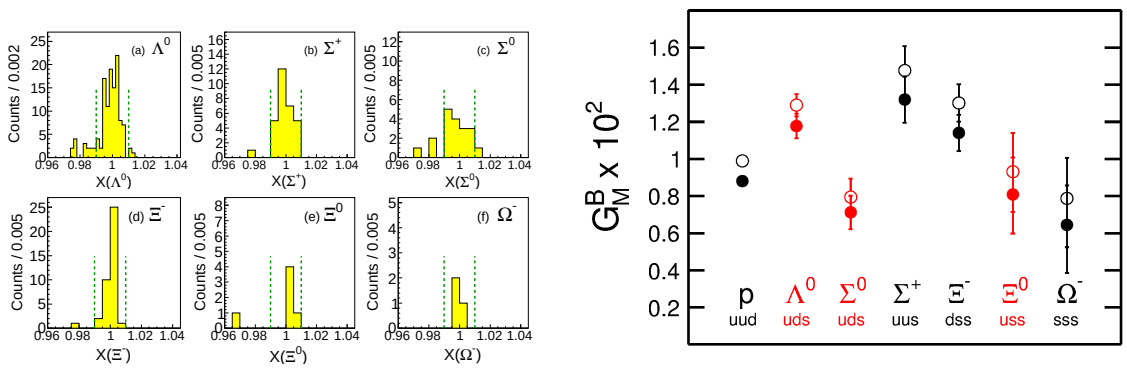

Figure 3. (left) Distributions of baryon-antibaryon scaled energy, $X(B) \equiv (E(B)+E(\overline{B}))/\sqrt{s}$, in $\sqrt{s} = 3770$ MeV data. The vertical lines indicate the signal region $X = 0.99 - 1.01$. (right) Magnetic form factors $|G_M^B| \times 10^2$ for protons and hyperons. The closed circles correspond to the assumption $G_M^B = G_E^B$, and the open circles to the assumption $G_E^B = 0$.

For the spin–1/2 baryons, the proton and the hyperons Λ, Σ, and Ξ, the well known relation between the cross sections and the magnetic form factor $G_M^B(s)$, and the electric form factor $G_E^B(s)$ is

$$\sigma_0^B = \left(\frac{4\pi\alpha^2\beta_B}{3s}\right)\left[|G_M^B(s)|^2 + (2m_B^2/s)|G_E^B(s)|^2\right] \tag{1}$$

where α is the fine structure constant, β_B is the velocity of the baryon in the center-of-mass system, and m_B is its mass. The statistics of the present measurements do not allow us to determine $|G_M^B|$ and $|G_E^B|$ separately. We therefore evaluate $|G_M^B(s)|$ under two commonly used extreme assumptions, $|G_E^B(s)|/|G_M^B(s)| = 0$, and 1. The results for $|G_E| = |G_M|$ are shown in Table 3. The efficiencies for the G_M and G_E components are determined assuming $1 + \cos^2\theta$ and $\sin^2\theta$ angular distributions, respectively. As shown in Fig. 3 (right), the values of $G_M^B(s)$ derived with the assumption $G_E^B = 0$ are found to all be nearly $\sim 12(2)\%$ larger than those for $G_E^B(s) = G_M^B(s)$.

The total systematic uncertainties from various sources are estimated to be 6.1% for Λ^0, 7.3% for Σ^0, 6,4% for Σ^+, 7.5% for Ξ^-, 7.3% for Ξ^0, and 10.2% for Ω^-.

Since no modern theoretical predictions for timelike form factors of hyperons at large momentum transfers exist, we can only discuss our experimental results qualitatively. Following are the main observations:

(a) The form factor cross sections in Table 3 are 150 to 500 times smaller than the resonance

Table 3. Results for proton and hyperon form factors at $|Q^2| = 14.2$ GeV^2, assuming $|G_E| = |G_M|$.

B	$N_{\rm ff}$	ϵ_B, %	σ_0^B, pb	$\lvert G_M^B\rvert\times 10^2$	$\lvert G_M^B/\mu_B\rvert\times 10^2$
p	215(15)	71.3	0.46(3)(3)	0.88(3)(2)	0.31(1)(1)
Λ^0	105(10)	21.1	0.80(8)(5)	1.18(6)(4)	1.93(9)(6)
Σ^0	15(4)	8.36	0.29(7)(2)	0.71(9)(3)	0.91(11)(3)
Σ^+	29(5)	4.68	0.99(18)(6)	1.32(13)(4)	0.54(5)(2)
Ξ^-	38(6)	8.69	0.71(11)(5)	1.14(9)(4)	1.75(14)(7)
Ξ^0	$5^{+2.8}_{-2.3}$	2.30	$0.35^{+0.20}_{-0.16}(3)$	0.81(21)(3)	0.65(17)(2)
Ω^-	$3^{+2.3}_{-1.9}$	2.94	$0.16^{+0.13}_{-0.10}(2)$	$0.64^{+0.21}_{-0.25}(3)$	$0.32^{+0.11}_{-0.13}(2)$

cross sections in Table 2.

(b) As illustrated in Fig. 3 (right), the measured values of $|G_M^B|$ vary rather smoothly by approximately a factor two, except for $G_M(\Sigma^0)$.

(c) As shown in Table 3, there is no evidence for the proportionality of $G_M^B(s)$ to μ_B for hyperons.

The most significant result of the present measurements is that $G_M(\Lambda^0)$ is a factor 1.66(24) larger than $G_M(\Sigma^0)$, although Λ^0 and Σ^0 have the same *uds* quark content. We note that Σ^0 and Λ^0 differ in their isospin, with $I(\Sigma^0) = 1$, and $I(\Lambda^0) = 0$. Since only up and down quarks carry isospin, this implies that the pair of up/down quarks in Λ^0 and Σ^0 have different isospin configurations. This forces different spin configurations in Λ^0 and Σ^0. In Λ^0 the *ud* quarks have antiparallel spins coupled to $S = 0$, whereas in Σ^0 they couple to $S = 1$. The spatial overlap in the $S = 0$ configuration in Λ^0 is stronger than in the $S = 1$ configuration in Σ^0, and our measurement at large $|Q^2|$ is particularly sensitive to it.

Recently, Wilczek and colleagues [4, 10, 11] have emphasized the importance of diquark correlations in low-energy QCD dynamics, and have pointed out that for the non-strange quarks the favorable diquark configuration with attraction is the spin-isospin singlet, making what Wilczek calls a "good" diquark in Λ^0 as opposed to the repulsive spin-isospin triplet configuration in Σ^0. This results in a significantly larger cross section for the formation of Λ^0 than Σ^0, as anticipated by Selem and Wilczek [11]. We measure $\sigma(\Lambda^0)/\sigma(\Sigma^0) \approx 3$, and this results in the factor 1.66 larger form factor for Λ^0 than Σ^0. We believe that our observation of the large difference in the form factors of Λ^0 and Σ^0 is indeed due to significant "good" diquark correlation in Λ^0, and it constitutes an important example of significant diquark correlations in baryons.

References

[1] N. Cabibbo and R. Gatto, Phys. Rev. Lett. **313**, 4 (1960); Phys. Rev. **124**, 1577 (1961).
[2] Kamal K. Seth *et al.*, Phys. Rev. Lett. **110**, 022002 (2013).
[3] B. Aubert et al. [BaBar Collaboration], Phys. Rev. D **76**, 092006 (2007).
[4] F. Wilczek, "Diquarks as Inspiration and as Objects", in "From Fields to Strings", ed. M. Shifman et al., World Scientific (Singapore), 2005, vol. 1, p. 77 – 93 [`arXiv:hep-ph/0409168`].
[5] J. G. Körner and M. Kuroda, Phys. Rev. D **16**, 2165 (1977).
[6] B. Aubert *et al.* [BaBar Collaboration], Phys. Rev. D **76**, 092006 (2007).
[7] J. Beringer *et al.* [Particle Data Group], Phys. Rev. D **86**, 010001 (2012) and 2013 partial update for the 2014 edition.
[8] G. Bonneau and F. Martin, Nucl. Phys. B **27**, 381 (1971).
[9] T. K. Pedlar *et al.* [CLEO Collaboration], Phys. Rev. D **72**, 051108 (2005).
[10] R. Jaffe and F. Wilczek, Phys. Rev. Lett. **91**, 232003 (2003).
[11] A. Selem and F. Wilczek, Proc. Ringberg Workshop on "New Trends in HERA Physics", ed. G. Grindhammer et al., World Scientific (Singapore), 2006, p. 337 – 356; [`arXiv:hep-ph/0602128`].